Origin Traceability of Medicinal *Astragalus Membranaceus* Based on LF-NMR Water-Absorption Kinetic Models and Multi-Level Confidence-Interval Scoring

Cheng Ni[1,2,#], Jin Chen[2,#], Jiarong Wang[3], Limin He[1,4,*], Jieru Cheng[3], Huiren Xu[1,*]
[1]*School of Intelligent Medicine and Technology, Hainan Medical University, Haikou, China*
[2]*School of Clinical Medicine, Hainan Medical University, Haikou, China*
[3]*The Second Clinical Medical College of Hainan Medical University, Haikou, China*
[4]*Key Laboratory of Tropical Translational Medicine of Ministry of Education, School of Public Health, Hainan Academy of Medical Sciences, Hainan Medical University, Haikou, China*
**Corresponding Author*
[#]*These authors contributed equally to this work*

Abstract: Conventional authentication of the geographical origin of *Astragalus membranaceus* usually depends on destructive extraction coupled with sophisticated instrumentation. In this work, an origin-traceability strategy was developed from water-absorption kinetics probed by low-field nuclear magnetic resonance (LF-NMR). Transverse-relaxation signals of samples from Gansu, Inner Mongolia, Shanxi and Yunnan were recorded continuously during water immersion, and the time-dependent total peak area per unit mass was fitted to four non-linear models (ExpDec2, ExpAssoc, ExpDec3 and Logistic), all giving coefficients of determination above 0.99. Because inter-model curve separation was most pronounced within the first 40 min, three time points (15, 20 and 30 min) were chosen as detection timestamps, and signal ranges bounded by the 95 %, 90 % and 85 % confidence intervals were combined into a graded scoring system (R = 1, 0.8, 0.3 and 0). Provenance-specific decision rules were then defined: dual-time-point (15 + 20 min) non-negative judgement for Gansu (ExpDec2) and Inner Mongolia (ExpDec3), dual-indicator (15 + 30 min) non-negative judgement for Shanxi (ExpAssoc), and a single-20 min positive judgement for Yunnan (Logistic). Blind tests on randomly selected batches gave detection accuracies of 100 %, 95 %, 95 % and 90 % for Gansu, Shanxi, Inner Mongolia and Yunnan, respectively. The workflow thus provides a pre-treatment-free, rapid and quantitative route for geographical-origin identification of herbal medicines.

Keywords: Origin Traceability; Low-Field Nuclear Magnetic Resonance; Kinetic Modelling; Confidence Interval; Graded Scoring; Blind Validation; Astragalus Membranaceus

1. Introduction

Astragalus membranaceus is a tonic herb widely used in traditional Chinese medicine, and verifying its origin has become a pressing quality-control issue: batches produced in different cultivation areas trade at markedly different prices and can differ in chemical composition [1,2]. Several analytical routes have been applied to herbal provenance discrimination, among them stable-isotope fingerprinting [2], laser-induced breakdown spectroscopy combined with Raman spectroscopy and deep-learning data fusion [3], portable Raman spectrometry coupled with partial-least-squares discriminant analysis [4], and chromatography-mass spectrometry profiling of malonyl-substituted flavonoid glycosides [5] or potential enzyme inhibitors [6,7]. Although these techniques are information-rich, most of them call for sample pre-treatment, skilled operators and long analysis times, which restricts their usefulness in the high-throughput screening of commercial batches.

Low-field nuclear magnetic resonance (LF-NMR) offers a non-destructive alternative: it probes the state and dynamics of water molecules inside intact biological matrices without any pre-treatment. In dried porous herbal materials, transverse-relaxation signals recorded during water uptake evolve with the

 Copyright @ STEMM Institute Press

internal pore structure, so material from different origins can be expected to leave distinguishable kinetic signatures. In the present study, time-resolved transverse-relaxation signals of A. membranaceus collected from four cultivation regions were converted into water-absorption kinetic models, and a multi-level confidence-interval scoring framework was used to turn model outputs into quantitative origin assignments. Three aims were pursued: (i) establishing provenance-specific non-linear kinetic models from LF-NMR time series; (ii) selecting characteristic detection timestamps and graded confidence-interval rules; and (iii) validating the resulting strategies with blind tests on randomly selected batches.

2. Materials and Methods

2.1 Materials

Dried roots of *Astragalus membranaceus* were obtained from Longxi (Gansu), Chifeng (Inner Mongolia), Datong (Shanxi) and Dali (Yunnan), which together cover the principal commercial cultivation zones of the herb in China. Before measurement, all samples were stored under dry conditions.

2.2 Instruments and Measurement Conditions

All relaxation measurements were carried out on a MesoMR23-060H-I low-field NMR analyser (0.5 T, 60 mm coil, 32 °C; Suzhou Niumag Electronic Technology Co., Ltd., China), and sample masses were recorded on an FS-1004 electronic balance. Transverse-relaxation data were collected with the CPMG pulse sequence, and T2 spectra were inverted with the Niumag magnetic-resonance signal software.

2.3 Acquisition of Transverse-Relaxation Signals

Each sample was placed into the probe coil and centred within the homogeneous region of the permanent magnet. After the Larmor frequency had been established by a hard-pulse free-induction-decay (FID) measurement, the CPMG pulse sequence was run to record T2-weighted echoes. Transverse-relaxation signals were acquired continuously over the entire water-uptake procedure, and the total peak area per unit mass derived from the inverted spectra at each sampling time was taken as the kinetic indicator.

2.4 Kinetic Model Construction

The dependence of the total peak area per unit mass on immersion time was fitted with four candidate non-linear models—ExpDec2, ExpAssoc, ExpDec3 and Logistic—using Origin 2022. For each origin, the optimal model was selected on the basis of the coefficient of determination (R2) and the visual agreement between the fitted curves and the experimental data.

2.5 Traceability Evaluation

For validation, five sample batches were drawn at random from each origin. The model that produced the largest signal separation at the characteristic time points of the kinetic curves was used for verification: measured signals were matched against the multi-level confidence-interval ranges, and the accuracy of each traceability strategy was evaluated at the corresponding detection timestamps.

3. Results and Discussion

3.1 Water-Absorption Kinetic Models from NMR Signals

Transverse-relaxation signals were recorded continuously for the four batches throughout water absorption, and non-linear curves relating immersion time to the total peak area per unit mass were constructed for each provenance (Figure 1).

The four models—ExpDec2, ExpAssoc, ExpDec3 and Logistic—were adopted selectively for the different sample groups, with the following mathematical expressions:

ExpDec2:

$$y = A_1 \times e^{-\frac{x}{t_1}} + A_2 \times e^{-\frac{x}{t_2}} + y_0 \quad (1)$$

ExpAssoc:

$$y = A_1 \times (1 - e^{-\frac{x}{t_1}}) + A_2 \times (1 - e^{-\frac{x}{t_2}}) + y_0 \quad (2)$$

ExpDec3:

$$y = A_1 \times e^{-\frac{x}{t_1}} + A_2 \times e^{-\frac{x}{t_2}} + A_3 \times e^{-\frac{x}{t_3}} + y_0 \quad (3)$$

Logistic:

$$y = A_2 + \frac{(A_1 - A_2)}{1 + \left(\frac{x}{x_0}\right)^p} \quad (4)$$

Every fitted model returned a coefficient of determination above 0.99, and the corresponding parameters are compiled in Table 1. As shown in Figure 1, the total peak area per unit mass of the Shanxi batch levelled off after 40 min, implying that its water-absorption

capacity was approaching saturation; the curves of the other three batches, by contrast, diverged markedly within the initial 40 min.

That four distinct models were needed for optimal fitting points to a deeper conclusion: geographical origin alters not only the rate at which water is absorbed but also the intrinsic kinetic mode of water ingress [1-3]. Within the first 40 min the total-peak-area-per-unit-mass values increased for every sample, yet a saturation plateau appeared only for the Shanxi batch. The Gansu, Inner-Mongolia and Yunnan batches kept rising without any observable inflection point, in line with the gravimetric observations reported in the companion physical-characterisation study of the same materials.

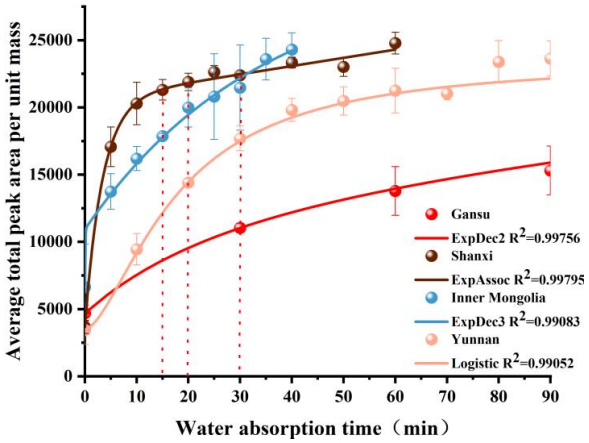

Figure 1. Magnetic Resonance Signal Variation Curve during the Water Absorption Process of Astragalus from Different Origins

Table 1. Parameters of the Water Absorption Dynamics Model

Water Absorption Dynamics Model	*ExpDec2*	*ExpAssoc*	*ExpDec3*	*Logistic*
y_0 or x_0	25482.20903	3666.32645	30257.90251	17.74693
A_1	-4920.21921	5.84142	-4180.96168	3481.48323
t_1	19.52637	9.53984	0.07205	
A_2	-15867.31386	16962.51575	-9485.07968	23523.41873
t_2	176.78632	3.37745	34.28764	
A_3			-9836.3786	
t_3			34.40808	
p				1.60548
R^2(COD)/%	99.756	99.795	99.083	99.052

3.2 Confidence-Interval-Graded Traceability Strategy

The magnetic-resonance signal of the Inner-Mongolia batch stabilised after 40 min of water absorption (Figure 2). During this fast-changing initial phase, three time points—15, 20 and 30 min—showed pronounced inter-model discrepancies and were therefore adopted as characteristic detection timestamps. Signal ranges bounded by the 95 % confidence intervals at these time points are listed in Table 2, and the corresponding 90 % and 85 % ranges in Tables 3 and 4, respectively.

Table 2. The Upper and Lower Limits of the 95% Confidence Interval of the Water Absorption Model

Model	*Water Absorption Time/min*	*Upper Limit*	*Lower Limit*
ExpDec2	15	7224.645	10021.955
	20	8398.455	10692.306
	30	10374.516	11691.136
ExpAssoc	15	20395.020	22304.794
	20	21147.354	22470.818
	30	22185.366	22738.276
ExpDec3	15	17174.789	18371.195
	20	17745.935	21182.620
	30	18623.313	25757.780
Logistic	15	11169.958	13145.732
	20	13903.652	15018.260
	30	16677.643	18306.578

Table 3. The Upper and Lower Limits of the 90% Confidence Interval of the Water Absorption Model

Model	*Water Absorption Time/min*	*Upper Limit*	*Lower Limit*
ExpDec2	15	7543.523	9757.083
	20	8673.806	10478.499
	30	10510.038	11555.614
ExpAssoc	15	20601.382	22098.432
	20	21290.362	22327.809
	30	22245.111	22678.531
ExpDec3	15	17367.023	18178.961
	20	18298.128	20630.426
	30	19769.651	24611.442
Logistic	15	11402.310	12960.823

 Copyright @ STEMM Institute Press

	20	*14018.381*	*14903.531*
	30	*16845.312*	*18138.908*

Table 4. The Upper and Lower Limits of the 85% Confidence Interval of the Water Absorption Model

Model	*Water Absorption Time/min*	*Upper Limit*	*Lower Limit*
ExpDec2	*15*	*7710.412*	*9590.194*
	20	*8809.869*	*10342.436*
	30	*10588.868*	*11476.784*
ExpAssoc	*15*	*20718.649*	*21981.165*
	20	*21371.628*	*22246.544*
	30	*22279.062*	*22644.580*
ExpDec3	*15*	*17455.732*	*18090.252*
	20	*18552.947*	*20375.608*
	30	*20298.649*	*24082.444*
Logistic	*15*	*11519.812*	*12843.321*
	20	*14085.115*	*14836.796*
	30	*16942.841*	*18041.379*

Each sample was graded by matching its measured signals against the multi-level confidence-interval ranges: R = 1 when the signal fell inside the 85 % range (positive, ++), R = 0.8 when it lay inside the 90 % but outside the 85 % range (weak positive, +), R = 0.3 when it fell within the 95 % but outside the 90 % range (weak negative, -), and R = 0 when no range was matched (negative, --).

The strategy makes full use of the rapidly varying 0-40 min kinetic interval, in which signals of different provenances diverge most (Figure 2); sampling at 15, 20 and 30 min guarantees sufficient inter-group distinction. The 85 %/90 %/95 % confidence-interval hierarchy replaces binary classification with graded scoring, with narrower ranges acting as stricter matching conditions: the 85 % interval is the strictest criterion for a positive assignment, whereas the 95 % interval sets the broadest boundary. The numerical scores (R = 0-1) thereby turn interval matching into computable indices suitable for automated decision-making [4-6].

Figure 2 summarises the detection outcomes for the four provenances. The ExpDec2 model, assigned to Gansu samples, achieved 100 % accuracy at all three timestamps (15, 20 and 30 min), and every off-target sample returned a negative result, which confirms the model's selectivity for Gansu material. Because the ExpDec2 curve stood well apart from the other model curves (Figure 2), sampling at 15 and 20 min simultaneously was adopted as the optimal Gansu scheme, striking a balance between a short assay time and high reliability.

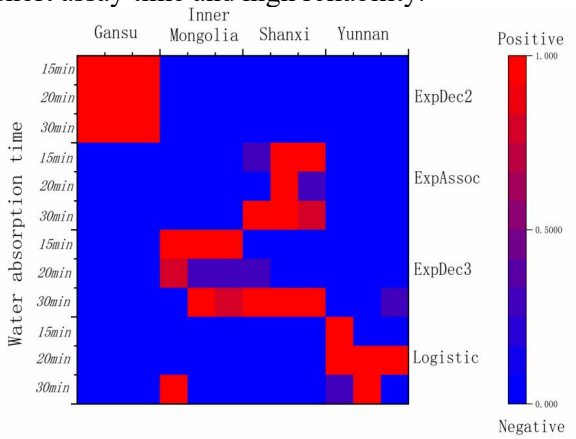

Figure 2. Distribution Map of Test Results for Astragalus from Different Origins.

For the ExpAssoc model assigned to Shanxi samples, all non-Shanxi samples produced negative outputs, so a negative result reliably rules out Shanxi as the origin of an unknown sample. Since some Shanxi samples gave weak-positive or weak-negative responses, a dual-indicator strategy requiring non-negative results at both the 15- and 30-min timestamps was adopted.

For the ExpDec3 model assigned to Inner-Mongolia samples, most target samples scored positive, although a subset gave weak-positive, weak-negative or negative results. Shanxi and Yunnan samples occasionally produced positive or weak-negative signals, particularly at 30 min. The ExpDec3-based strategy accordingly demands non-negative outputs at both 15 and 20 min before a positive assignment is made.

The Logistic model missed a substantial fraction of Yunnan samples, and its performance was worst at 15 min; acceptable accuracy was reached only at 20 min, where the fitted curve deviated most from the other model trajectories (Figure 2). The Logistic-based workflow therefore rests solely on the 20-min timestamp, and a positive result there is diagnostic of Yunnan provenance.

The performance limitations of the four models differed from origin to origin. ExpDec2 achieved perfect specificity and accuracy at several time points because of its well-separated kinetic profile and needed only dual-time-point sampling. ExpAssoc and ExpDec3 exhibited partial deviations of the target samples and occasional cross-signal interference, so joint judgement at two time points was necessary to

Copyright @ STEMM Institute Press

reduce false positives and false negatives. Logistic was strongly time-dependent: reliable discrimination was limited to the 20-min window and deteriorated sharply outside it.

Discriminative performance paralleled the inter-curve separation visible in Figure 2, from which two generalised rules emerge: single-time-point identification is feasible only when the model curves are sufficiently differentiated, and multi-time-point combined evaluation becomes indispensable when signals overlap across provenances. Together these observations provide practical analytical rules for LF-NMR-based geographical-origin discrimination of A. membranaceus [5-8].

3.3 Blind Validation of the Traceability Strategies

Five batches per origin were selected at random for blind testing, and the results are summarised in Table 5. The ExpDec2-based strategy achieved 100 % detection accuracy for Gansu samples, while the ExpAssoc (Shanxi), ExpDec3 (Inner Mongolia) and Logistic (Yunnan) strategies reached 95 %, 95 % and 90 %, respectively.

Table 5. Results of Strategy Validation

Sample	*ExpDec2*			*ExpAssoc*			*ExpDec3*			*Logistic*
	15min	*20min*		*15min*	*30min*		*15min*	*20min*		*20min*
Gansu A	+ +	+ +		- -	- -		- -	- -		- -
Gansu B	+ +	+ +		- -	- -		- -	- -		- -
Gansu C	+ +	+ +		- -	- -		- -	- -		- -
Gansu D	+ +	+ +		- -	- -		- -	- -		- -
Gansu E	+ +	+ +		- -	- -		- -	- -		- -
Shanxi A	- -	- -		+ +	+ +		- -	- -		- -
Shanxi B	- -	- -		+ +	-		- -	- -		- -
Shanxi C	- -	- -		+ +	+		- -	- -		- -
Shanxi D	- -	- -		- -	- -		- -	- -		- -
Shanxi E	- -	- -		+ +	+ +		- -	- -		- -
Inner Mongolia A	- -	- -		- -	- -		+ +	+		- -
Inner Mongolia B	- -	- -		- -	- -		+ +	-		- -
Inner Mongolia C	- -	- -		- -	- -		- -	-		- -
Inner Mongolia D	- -	- -		- -	- -		+ +	-		- -
Inner Mongolia E	- -	- -		- -	- -		- -	+ +		- -
Yunnan A	- -	- -		- -	- -		- -	-		+ +
Yunnan B	- -	- -		- -	- -		- -	- -		+ +
Yunnan C	- -	- -		- -	- -		- -	- -		+ +
Yunnan D	- -	- -		- -	- -		- -	- -		+ +
Yunnan E	- -	- -		- -	- -		- -	+		- -

A head-to-head comparison across the validation datasets discloses a clear performance gradient. ExpDec2 delivered error-free classification, consistent with its perfect selectivity in the model-performance tests. ExpAssoc and ExpDec3 both reached 95 % accuracy, and their slight shortfall relative to ExpDec2 matches their partial weak-positive or weak-negative responses and occasional cross-interference. Logistic recorded the lowest accuracy (90 %), in agreement with the risk of missed detection outside the narrow 20-min window.

All four strategies recognised their target provenances with acceptable selectivity, showing that the multi-time-point, confidence-interval-graded rules transfer well to randomly sampled specimens. The descending accuracy order (Gansu > Shanxi ≈ Inner Mongolia > Yunnan) is consistent with the degree of kinetic-curve separation: the larger the inter-model separation, the higher the practical accuracy, while partial signal overlap explains the limited misclassification events [7-9]. These blind tests verify that the LF-NMR-driven framework is workable for the geographical-origin discrimination of A. membranaceus [10,11].

4. Discussion

4.1 Principal Results

Time-resolved LF-NMR transverse-relaxation signals were converted into provenance-specific water-absorption kinetic models for A.

 Copyright @ STEMM Institute Press

membranaceus, and the model outputs were translated into a graded, quantitative origin-traceability framework. Four non-linear models were needed to represent the four batches, all with coefficients of determination above 0.99, which indicates that the kinetic form itself is sensitive to origin. The 0-40 min fast-variation window proved the most informative stage, and the combination of three timestamps (15, 20 and 30 min) with the 85 %/90 %/95 % confidence-interval hierarchy allowed graded scoring without the rigidity of binary classification. Blind validation confirmed that the rules transfer across batches, with accuracies of 100 % (Gansu), 95 % (Shanxi), 95 % (Inner Mongolia) and 90 % (Yunnan).

4.2 Limitations

Four limitations deserve mention. First, the dataset covers only four representative origins and excludes other cultivars, harvest years, cultivation modes and storage conditions [1-2], so generalisability to a broader cohort remains untested. Second, partial overlap among kinetic curves creates a risk of misclassification, as reflected in the lower accuracy for Yunnan samples, whose Logistic model depends heavily on the narrow 20-min window. Third, discrimination relies on microstructural water-transport differences without incorporating metabolomic or phytochemical fingerprints, which may limit performance for microstructurally similar samples. Future studies should enlarge the sample library, fuse LF-NMR data with chromatographic or metabolomic datasets in multi-source models, relax the strict time-window dependence, and carry out simulated-field and pilot-industrial validation in quality-control settings of the traditional-Chinese-medicine industry [3].

4.3 Comparison with Prior Work

Conventional provenance-identification studies of A. membranaceus rely predominantly on chromatographic, spectroscopic and metabolomics-oriented methodologies that quantify characteristic secondary metabolites for quality and origin assessment [3-7]. These approaches deliver reliable compositional information but commonly require complicated pre-processing, lengthy procedures and chemical reagents. The LF-NMR-driven strategy presented here avoids destructive pre-treatment and acquires data rapidly by detecting proton-based water-status signals from internal porous microstructures. Unlike the static single-point measurements reported in most existing LF-NMR studies of herbal quality, the present work records dynamic time-series signals over the whole water-absorption procedure, builds origin-specific non-linear kinetic models, and proposes hierarchical confidence-interval-scoring traceability strategies with quantitative blind-batch validation. Because the method does not measure active phytochemical constituents directly, it cannot replace chromatographic or metabolomic techniques when detailed compositional profiling is required; instead, it complements them, with microstructural LF-NMR kinetic features serving as preliminary high-throughput screening indicators and suspicious samples confirmed by compositional assays. Provenance discrimination that combines dynamic LF-NMR water-uptake kinetics has rarely been reported, and the present work offers an alternative non-destructive route for authenticating porous-matrix medicinal plants, which can be extended to other herbal species in future research [1].

5. Conclusion

A geographical-origin traceability methodology for A. membranaceus based on LF-NMR was developed through water-absorption kinetic characterisation. Four non-linear kinetic models (ExpDec2, ExpAssoc, ExpDec3 and Logistic) were built from transverse-relaxation time series, and multi-time-point, confidence-interval-graded discrimination strategies were designed for the four producing regions. Blind validation on randomly selected batches gave accuracies of 100 % (Gansu), 95 % (Shanxi and Inner Mongolia) and 90 % (Yunnan). Greater separation among the kinetic curves corresponded to higher identification reliability, whereas overlapping signals called for joint judgement at multiple timestamps. The method avoids complex sample pre-processing and offers a technical reference for rapid origin traceability and quality assessment of A. membranaceus, and it can also serve as a framework for authenticating other porous-matrix medicinal herbs.

Acknowledgment

This work was financially supported by the Entrepreneurship and Innovation Project of Hainan Medical University (S202411810012),

Copyright @ STEMM Institute Press

the Cooperative Education Project of the Ministry of Education (No. 241205876191733, No. 250601416251501), the Academic Enhancement Support Program of Hainan Medical University (XSTS2026180) and the research start-up fund of Hainan Medical University.

References

[1] Hu X.Y., Qie M.J., Zhao S.S., et al. Research progress on the application of analytical techniques in the traceability of the origin and authentication of traditional Chinese medicines. Journal of Anhui Agricultural Sciences, 2023, 51(4): 16-20. (in Chinese)

[2] Ming L.L., Fan Z.L., Wang H.Y., et al. Determination of carbon and nitrogen isotope ratios in Astragalus membranaceus by elemental analysis-isotope ratio mass spectrometry and its application in origin traceability. Chemical Industry Times, 2021, 35(5): 18-21. (in Chinese)

[3] Ren L.H., Wang F.C., Zhang Y.L., et al. Rapid identification of Radix Astragali by data fusion of laser-induced breakdown spectroscopy and Raman spectroscopy coupled with deep learning. Talanta, 2025, 282: 127016.

[4] Lu H.Z., Wang Y., Zhu J.Y., et al. Rapid analysis of Radix Astragali using a portable Raman spectrometer with 1064-nm laser excitation and data fusion with PLS-DA. Spectrochimica Acta Part A: Molecular and Biomolecular Spectroscopy, 2024, 313: 124087.

[5] Guo Y.X., Li Y.Y., Wang Y.K., et al. A combination screening strategy based on UPLC-HRMS and UPLC-MRM for the comprehensive analysis of malonyl-substituted flavonoid glycosides in Astragalus. Journal of Chromatography A, 2025, 1739: 465548.

[6] Wang H.P., Lin Z.Z., Zhao C., et al. Screening of potential alpha-glucosidase inhibitors from Astragalus membranaceus by affinity ultrafiltration screening coupled with UPLC-ESI-Orbitrap-MS method. Journal of Asian Natural Products Research, 2024, 26(11): 1348-1357.

[7] Abdallah I.I., Shawky E., Mustafa R., et al. UPLC-MS/MS based metabolomic insights into antidiabetic potential of Astragalus: deciphering species-specific bioactive metabolites in correlation to alpha-amylase and alpha-glucosidase inhibitory activities. Microchemical Journal, 2025, 208: 112481.

[8] Lankhorst P., Chang A.N. The application of NMR in compositional and quantitative analysis of oils and lipids.Modern Magnetic Resonance. Cham: Springer, 2017: 1-22.

[9] Ozel B., Oztop M.H. A quick look to the use of time domain nuclear magnetic resonance relaxometry and magnetic resonance imaging for food quality applications. Current Opinion in Food Science, 2021, 41: 122-129.

[10] Zhang Y., Zhao Y.N., Zhao J.X., et al. Detection and discrimination of soybean oil content based on low-field nuclear magnetic resonance technology with various dimensions. Transactions of the Chinese Society of Agricultural Engineering, 2024, 40(4): 337-344. (in Chinese)

[11] Jiang X.M., Yang D.H., Xiang G.Q., et al. Determination of cis/trans fatty acid contents in edible oils by 1H NMR spectroscopy in association with multivariate calibration. Journal of Food Composition and Analysis, 2022, 105: 1041.

 Copyright @ STEMM Institute Press